Assessing Interannual Variation in MODIS-Based Estimates of Gross Primary Production

David P. Turner, William David Ritts, Maosheng Zhao, Shirley A. Kurc, Allison L. Dunn, Steven C. Wofsy, Eric E. Small, and Steven W. Running

***Abstract*—Global estimates of terrestrial gross primary production (GPP) are now operationally produced from Moderate Resolution Imaging Spectrometer (MODIS) imagery at the 1-km spatial resolution and eight-day temporal resolution. In this study, MODIS GPP products were compared with ground-based GPP estimates over multiple years at three sites—a boreal conifer forest, a temperate deciduous forest, and a desert grassland. The ground-based estimates relied on measurements at eddy covariance flux towers, fine resolution remote sensing, and modeling. The MODIS GPP showed seasonal variation that was generally consistent with the *in situ* observations. The sign and magnitude of year-to-year variation in the MODIS products agreed with that of the ground observations at two of the three sites. Examination of the inputs to the MODIS GPP algorithm—notably the fraction of photosynthetically active radiation (FPAR) that is absorbed by the canopy), minimum temperature scalar, and vapor pressure deficit scalar—provided explanations for cases of disagreement between the MODIS and ground-based GPP estimates. Continued evaluation of interannual variation in MODIS products and related climate variables will aid in assessing potential biospheric feedbacks to climate change.**

***Index Terms*—Fraction of photosynthetically active radiation (FPAR), global ecology, gross primary production (GPP), interannual variation, modeling, Moderate Resolution Imaging Spectrometer (MODIS), remote sensing.**

I. Introduction

INTEREST in the interannual variation in global gross primary production (GPP) and net primary production (NPP) is driven in part by the need to understand potential biospheric feedbacks to climate change. GPP is the rate of carbon fixation or gross assimilation per unit ground surface area, whereas NPP is the rate of biomass accumulation per unit ground surface area [1], [2]. In a sense, each year is a massive natural experiment and differences in biosphere behavior between relatively cool years (e.g., those following the eruption of Mt. Pinatubo) and relatively warm years (e.g., 1998) are informative with respect to predicting carbon fluxes. To take advantage of these experiments, year-specific global GPP/NPP and climate must be accurately monitored [3]. At present, much more is known about interannual variation in global climate than about interannual variation in global NPP and GPP. However, satellite-borne sensors such as AVHRR, SeaWIFS, VEGETATION, and the Moderate Resolution Imaging Spectrometer (MODIS) now achieve daily coverage of the Earth's surface at 1-km resolution or less and offer the opportunity for greatly improved monitoring of biospheric carbon fluxes [4].

To be scientifically useful, spatial and temporal patterns in global flux estimates inferred from satellite data will require evaluation based on *in situ* measurements [5], [6]. GPP can be monitored from measurements of net ecosystem exchange at eddy covariance flux tower sites [7], but a host of scaling issues arise in linking tower measurements to satellite-based flux estimates [8]. The BigFoot Project (http://www.fsl.orst.edu/larse/bigfoot/index.html) was designed specifically to address many of these scaling issues and to evaluate MODIS land products using ground measurements. The NASA MODIS Land Science Team now produces global estimates of mean GPP every eight days for each 1 km^2 of the land surface [4]. This paper focuses on assessing interannual variation in the MODIS GPP product at three of the BigFoot sites.

The MODIS GPP algorithm (MOD17) uses data from MODIS surface reflectances. That data contains information about vegetation phenology and canopy absorbance of photosynthetically active radiation or the fraction of photosynthetically active radiation (FPAR) [9], [10]. MOD17 also uses climate data from the NASA Data Assimilation Office (DAO) climate model [11]. Particularly, important within the DAO data stream is the estimate of incident photosynthetically active radiation ($\downarrow$ PAR). In MOD17, the product of $\downarrow$PAR and FPAR is the absorbed PAR (APAR). To estimate GPP, a maximum light use efficiency (LUE) for GPP (ε_{g-max}) from a biome-specific lookup table [12] is first modified by scalars (0–1) for minimum temperature ($S_{T\,min}$) and vapor pressure deficit (S_{VPD}), i.e., ε_{g-max} is reduced under unfavorable conditions. GPP is then the product of APAR ($MJ \cdot m^{-2} \cdot d^{-1}$) and LUE ($gC \cdot MJ^{-1}$). This algorithm should in principle detect effects of interannual variation in spring snow melt, in leaf phenology, and in responses of grasslands to increased precipitation. However, few studies have documented these capabilities. Here, we evaluate the interannual variation in MODIS-based GPP at three sites varying widely in climate, productivity, and vegetation physiognomy.

Manuscript received October 1, 2004; revised January 23, 2006. This work was supported in part by the National Aeronautics and Space Administration (NASA) Terrestrial Ecology Program and in part by the Department of Energy, NASA, and the National Science Foundation (for the Flux tower measurements).

D. P. Turner and W. D. Ritts are with the Department of Forest Science, Oregon State University, Corvallis, OR 97331 USA (e-mail: david.turner@oregonstate.edu).

M. Zhao and S. W. Running are with the School of Forestry, University of Montana, Missoula, MT 59812 USA.

S. A. Kurc and E. E. Small are with the Department of Geological Sciences, University of Colorado, Boulder, CO 80309 USA.

A. L. Dunn and S. C. Wofsy are with the Department of Earth and Planetary Science, Harvard University, Cambridge, MA 02138 USA.

Digital Object Identifier 10.1109/TGRS.2006.876027

TABLE I
SITE LOCATION AND LONG-TERM AVERAGE CLIMATE VARIABLES

Code	Vegetation	Location	Precipitation (cm)	MAT[a] (°C)
NOBS	Boreal Forest	Lat: 55.885260 Lon: -98.477268	52	-3.20
HARV	Deciduous Forest	Lat: 42.528513 Lon: -72.172907	111	8.31
SEVI	Desert Grassland	Lat: 34.350858 Lon: -106.689897	35	13.57

[a] Mean Annual Temperature

II. METHODS

A. Sites

The three BigFoot sites were used in this study were the boreal forest site (NOBS), the temperate deciduous forest site (HARV), and the desert grassland site (SEVI). Site locations and long-term average temperature and precipitation are listed in Table I. The NOBS site is a boreal black spruce (*Picea mariana*) forest in northern Manitoba Canada. NOBS was one of the core sites in the NASA-sponsored BOREAS Study [13]–[15]. The HARV site is in eastern Massachusetts and is dominated by northern hardwoods, including *Quercus rubra*, *Acer rubrum*, and *Fraxinus Americana*. The Harvard Forest eddy covariance tower [16] is located near the center of the study area. The SEVI site is in the Sevilleta Long Term Ecological Research study area in south central New Mexico [17]. Vegetation is predominantly perennial bunchgrasses, dominated by Black Grama (*Bouteloua eriopoda*) and Blue Grama (*Bouteloua gracilis*), along with sparse annual grasses, forbs, and cacti.

B. MODIS Products

The MODIS data stream includes estimates of FPAR, leaf area index (LAI), and GPP at the 1-km resolution. The values are eight-day maxima in the case of FPAR and LAI, and eight-day means for GPP. Related inputs to the MOD17 algorithm are daily ↓PAR, minimum temperature (Tmin), average temperature (Tavg), and vapor pressure deficit (VPD). This study employed version 4.5 of the MODIS GPP products and related inputs [18]. In version 4.5, missing and bad quality labeled values in the Collection 4 LAIs and FPARs [19] were filled by linear interpolation within each year and the meteorological inputs from the DAO climate model were interpolated to the 1-km resolution from their native $1^\circ \times 1.25^\circ$ resolution. Missing FPAR data through Day 57 of the year 2000 were filled by the average values of FPAR for the same periods for 2001–2003.

C. BigFoot Products

The BigFoot Project was designed specifically to evaluate MODIS Land products [8], [20], [21]. At each BigFoot site, a 25-km^2 study area is established which contains an eddy covariance flux tower [22]. One hundred plots are laid out within that study area and seasonal measurements of LAI are made at each plot. Measurements of above-ground net primary production are made at half the plots and total NPP is estimated for each of these plots using vegetation-type-specific ratios of belowground production to above-ground NPP [23]. Scaling of LAI over the complete study area is based on empirical relationships of measured LAIs to spectral vegetation indexes from Landsat data [24]–[26]. Scaling GPP and NPP is done by running the Biome-BGC ecosystem process model at each 25-m grid cell. A 25-m grid was used because 25 m is close to the resolution of the Landsat data, and it captures the significant fine scale heterogeneity in vegetation properties at several of the BigFoot sites. Biome-BGC is a daily time step model that simulates photosynthesis, plant respiration, and site water balance [27], [28]. The daily climate inputs to the model are from the meteorological measurements at the flux towers. BigFoot estimates of NPP (based on measured above-ground NPP) are used in model calibration.

GPP estimates from the flux tower are used to evaluate the effectiveness of the BigFoot products in capturing seasonality, maximum values, and annual totals for GPP [8]. Tower GPP is estimated from measurements of net ecosystem exchange (NEE) using the relationship

$$\mathrm{GPP} = \mathrm{NEE} - \mathrm{R_e}$$

where $\mathrm{R_e}$ is ecosystem respiration (the sum of autotrophic and heterotrophic respiration). This calculation is made for each half hour during the daylight periods. The $\mathrm{R_e}$ estimate is based on the air or soil temperature and the relationship of NEE to air or soil temperature during nighttime periods above a threshold friction velocity [7], [8]. A separate relationship is established for each of several intervals during the growing season. Uncertainty in the GPP estimates at the HARV site are discussed in Goulden *et al.* [7]. Note that possible systematic errors such as overestimation of daytime $\mathrm{R_e}$ [29] would not influence the ability to detect the sign of the change in total GPP from year to year.

The flux tower footprint, i.e., the area over which the signal is integrated, varies temporally depending on factors such as wind speed and direction. For the comparisons of tower GPP and BigFoot GPP, the footprint was crudely approximated as the area within a 0.5-km radius of the tower [30]. Thus, BigFoot GPPs for all 25-m cells within that 0.7-km^2 area were averaged for the purposes of comparisons with tower GPPs.

An important feature of the BigFoot protocol as related to interannual variation is that LAI is comprehensively prescribed spatially and temporally in the Biome-BGC model runs. Biome-BGC is most commonly run in a prognostic mode, i.e., LAI is self-regulated. However, to maximize the benefits of the BigFoot LAI measurements, the internal phenology and allocation algorithms were turned off in the BigFoot application and LAI was prescribed. Comparison of BigFoot surfaces for LAI and annual GPP (Fig. 1) show the strong influence of LAI on the GPP estimate.

A unique seasonal LAI trajectory for each 25-m grid cell in a given year was derived from the mid-growing season maximum LAI, as estimated from Landsat data, and a reference trajectory (i.e., template) based on field observations. At HARV, above- and below-canopy PAR sensors at the tower were used

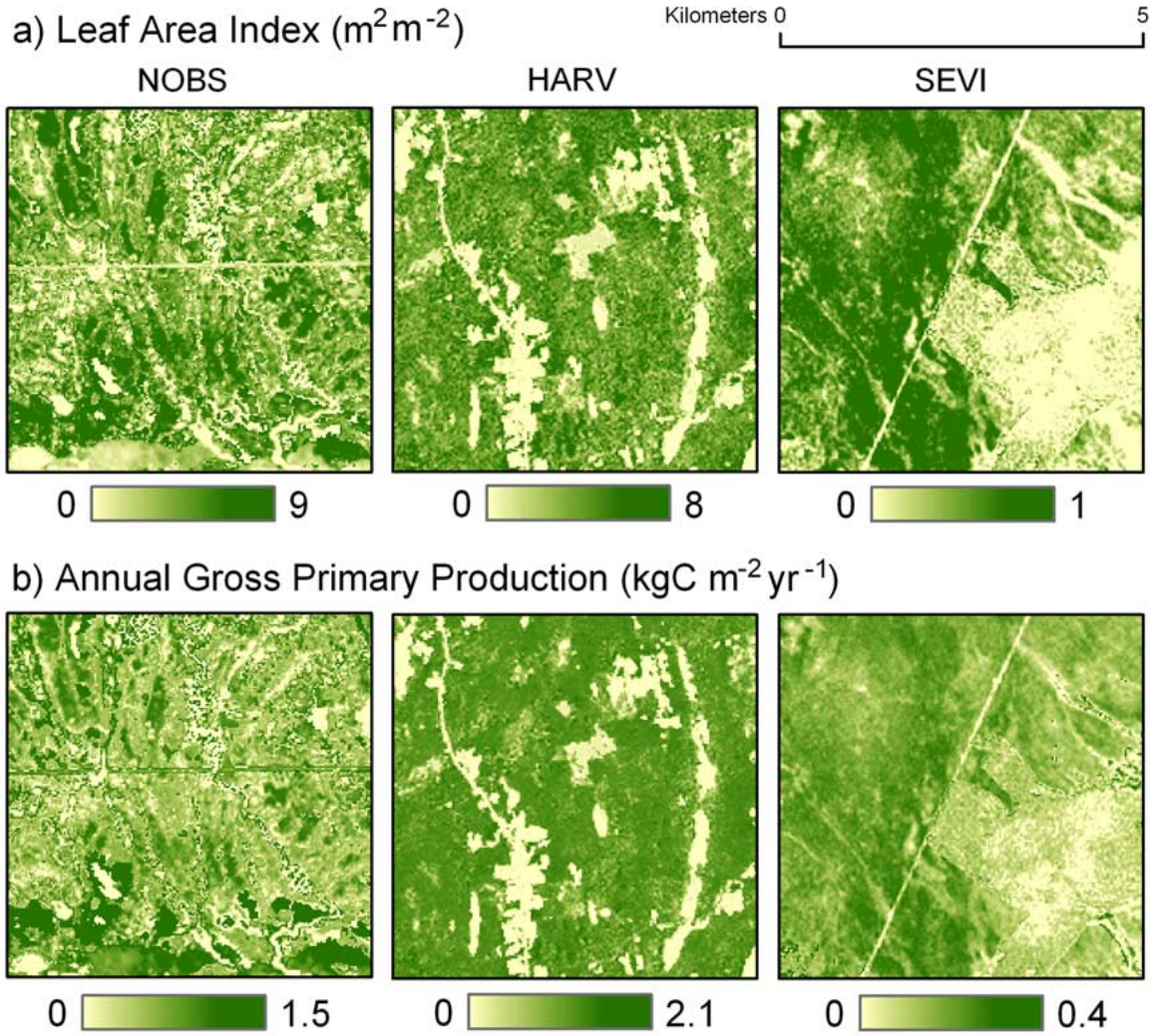

Fig. 1. Comparison of (a) leaf area index and (b) gross primary production at the three study sites.

to monitor transmittance and a simple Beer's Law formulation converted transmittance to an estimate of LAI [31]. An interpolation to the daily time step was made from weekly LAI estimates. These transmittance-based LAI trajectories showed good agreement with the direct observations of leaf phenology at the site [31], [32]. At SEVI, the template was based on the monthly measurements of LAI. The template for the conifer cover types was a constant set at the mean value from the field LAI measurements. Leaf-on and leaf-off for deciduous species at NOBS was assumed to be Day of Year (DOY) 130 and DOY 270, respectively [33]. Given the template (covering 365 days) and the Landsat-based LAI at mid-growing season, the ratio of the LAI at the 25-m cell to the template LAI on the day of the Landsat scene acquisition was determined. That ratio was then applied to the template LAI for each day of the year to generate the cell-specific LAI trajectory.

At HARV, field measurements of LAI and associated Landsat LAI surfaces were made in 2000, 2001, and 2002. For logistical reasons new maximum LAI measurement were not made in 2004. However, there was not much interannual variation in maximum leaf area, i.e., the difference in mean LAI over the site between 2001 and 2002 was less than 10% [26]. The above- and below-canopy PAR measurements at HARV were made during each of the four years and were the basis for the year-specific reference LAI trajectories. The land cover map used to initialize the Biome-BGC model was updated in 2002 at HARV to reflect a small logging event. At the NOBS site, the land cover as well as the maximum LAI was held constant over the four-year study period. At SEVI, land cover and LAI were updated from 2002 to 2003.

D. Comparisons

Comparisons of MODIS and BigFoot data are presented in the form of mean values over the 25 1-km^2 MODIS cells at a site. To achieve precise spatial correspondence, BigFoot data at the 25-m resolution were reprojected from the UTM coordinate system to the Sinusoidal coordinate system native to the MODIS products [25]. BigFoot data were then overlain with the MODIS grid and values for the 25-m cells were averaged within each 1-km MODIS cell. To achieve temporal correspondence, the BigFoot daily GPPs were aggregated to the eight-day bins associated with the MODIS GPP product. To aid in the GPP and FPAR comparisons, an indication of the beginning and end of the growing season was determined from observations at the

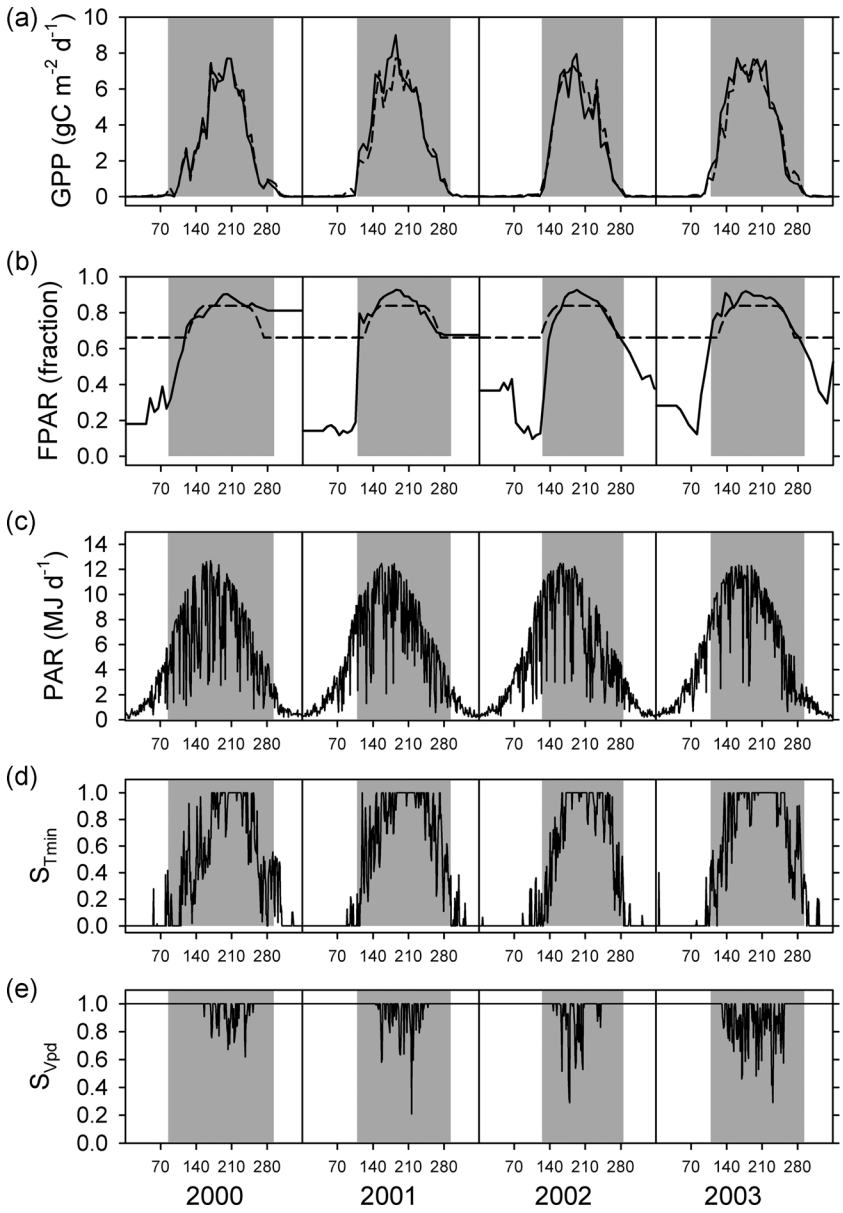

Fig. 2. Time course of (a) GPP and (b) FPAR for (dashed) MODIS and (solid) BigFoot at the NOBS site along with associated (c) ↓PAR, (d) $S_{T\,min}$, (e) and S_{VPD}. Values for GPP and FPAR are at eight-day means and represent the average over 25 1-km^2 MODIS cells. ↓ PAR, $S_{T\,min}$, and S_{VPD} are reported as daily values. The shading indicates the growing season, here defined by the first and last day that flux tower GPP achieved a value of 1 gC $\cdot$ m^{-2} $\cdot$ d^{-1}.

eddy covariance flux towers. Criteria used for these dates were the first and last days of the year that GPP rose above 1 gC $\cdot$ m^{-2} $\cdot$ d^{-1}. Total annual GPP at the flux towers was also calculated for each year.

III. Results

Comparisons here and in previous studies [8], [21] of the seasonality and absolute magnitude of BigFoot GPP products and GPP indicated by an eddy covariance flux towers have found generally good agreement at the three study sites. For the year of eight-day bins in 2002, the Pearson's correlation coefficients for the eight-day mean GPPs were 0.98, 0.97, and 0.89 at NOBS, HARV, and SEVI, respectively. Annual GPP over the footprint differed by 21% at NOBS, 7% at HARV, and 7% at SEVI. Both flux tower and BigFoot products indicated a relatively late beginning and early end of the growing season at NOBS in 2002, a relatively early spring rise in GPP at HARV in 2001 (achieving 6 gC $\cdot$ m^{-2} $\cdot$ y^{-1} by DOY 140), and a delayed beginning of the growing season at SEVI in 2003. With the exception of 2002 to 2003 at the HARV site, there was consistent agreement between flux tower and BigFoot products with regard to the year-to-year changes in sign for total GPP. Inspection of the land cover map at the sites shows that the 0.7 km^2 around the flux tower was reasonably representative of the vegetation cover over the 25-km^2 study area in each case, thus lending confidence to the BigFoot flux estimates over the entire study area.

In comparisons of the MODIS and BigFoot GPP products at the NOBS site, the two approaches gave similar results for the beginning and end of the growing season [Fig. 2(a)]. The

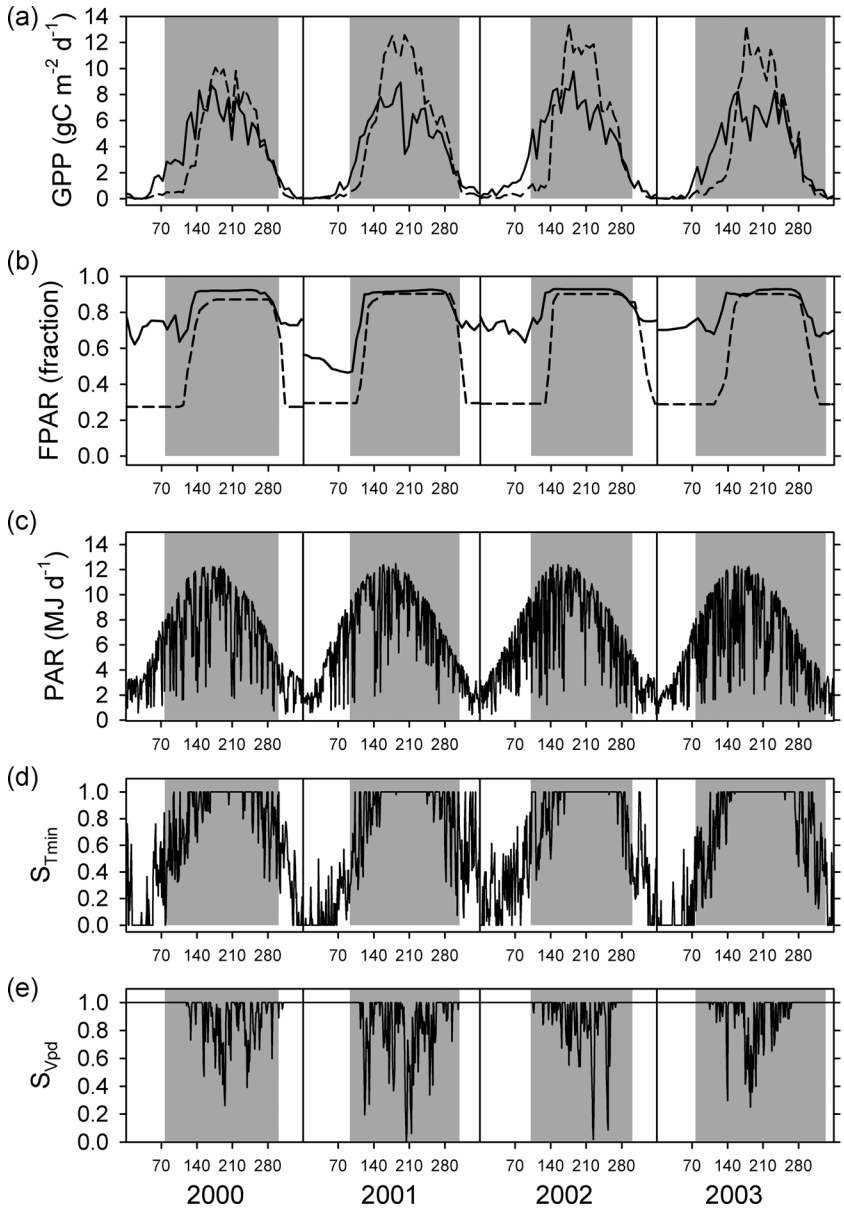

Fig. 3. Time course of (a) GPP and (b) FPAR for (dashed) MODIS and (solid) BigFoot at the HARV site along with associated (c) ↓PAR,(d) $S_{T\,min}$, and (e) S_{VPD}. Values for GPP and FPAR are at eight-day means and represent the average over 25 1-km^2 MODIS cells. ↓PAR, $S_{T\,min}$, and S_{VPD} are reported as daily values. The shading indicates the growing season, here defined by the first and last day that flux tower GPP achieved a value of 1 $gC \cdot m^{-2} \cdot d^{-1}$.

distinctively short growing season in 2002 resulted from a relatively late spring, and that effect was clearly captured by the MODIS algorithm. It is the $S_{T\,min}$ in particular that drives the seasonality of the MODIS GPP at NOBS [Fig. 2(d)]. The MODIS FPAR has significant errors outside the growing season at NOBS [Fig. 2(b)], but these did not have much of an impact on estimated GPP at the beginning and end of the growing season because of the strong control on GPP by $S_{T\,min}$. The absolute magnitude of the total GPP, as well as the sign of the year-to-year change in total GPP was the same for the BigFoot and MODIS products, but the magnitude of the interannual variation in total GPP was greater for the MODIS estimates than for the BigFoot estimates (Fig. 5).

At the HARV site, the MODIS GPP indicated an earlier beginning of the growing season than did the BigFoot product for all four years [Fig. 3(a)]. There was greater consistently with regard to the end of the growing season. The discrepancy at the beginning of the growing season is driven primarily by the high FPAR seen in the MODIS products even outside the growing season [Fig. 3(b)]. With the high FPAR, GPP is initiated in the MODIS algorithm as soon as temperatures warm significantly. This response does not account for a lag in several weeks for bud break and leaf out. There is a substantial rise in MODIS FPAR about the same time as the BigFoot FPAR rises and it appears to be closely related to the actual increase in green foliage. The relatively late spring recovery of GPP in 2002 at the HARV site is not seen in the MODIS GPP. The sign of the year-to-year changes in total GPP for the MODIS products was not consistent with that of the BigFoot products (Fig. 5) and the magnitude of the interannual differences was muted in the MODIS products. The similarity in absolute magnitude of total GPP between the MODIS and BigFoot products was because of counteracting er-

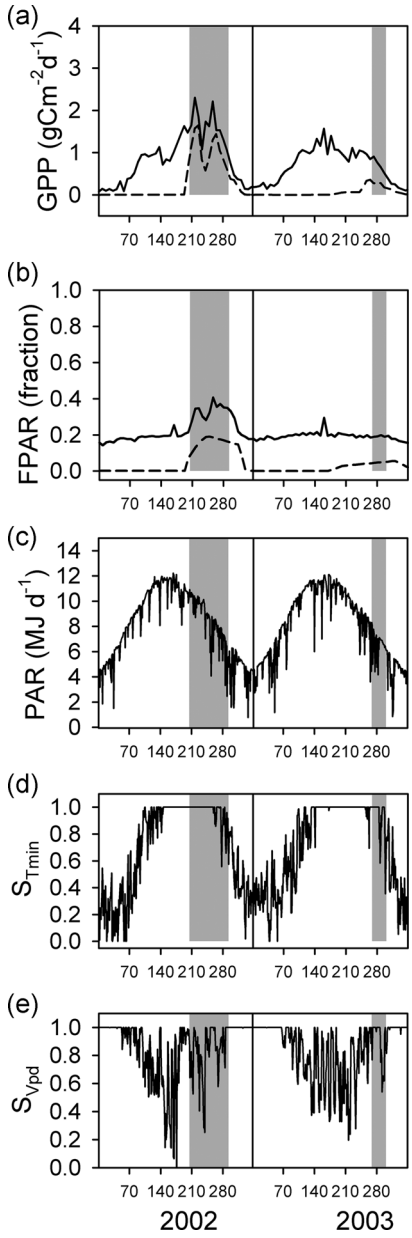

Fig. 4. Time course of (a) GPP and (b) FPAR for (dashed) MODIS and (solid) BigFoot at the SEVI site along with associated (c) ↓PAR,(d) $S_{T\,min}$, and (e) S_{VPD}. Values for GPP and FPAR are at eight-day means and represent the average over 25 1-km^2 MODIS cells. ↓PAR, $S_{T\,min}$, and S_{VPD} are reported as daily values. The shading indicates the growing season, here defined by the first and last day that flux tower GPP achieved a value of 1 gC $\cdot$ m^{-2} $\cdot$ d^{-1}.

rors in the MODIS product [8], i.e., values too high in the spring and too low in mid-growing season.

At the SEVI site, we had only two years of observations but the two years differed strongly with respect to precipitation, i.e., there was much less precipitation in 2003 (120 mm) than 2002 (247 mm) and it arrived later in the year. The BigFoot GPP first reached above 1.0 gC $\cdot$ m^{-2} $\cdot$ d^{-1} on DOY 211 in 2002 (in agreement with flux tower data [21]), but did not rise above 1.0 gC $\cdot$ m^{-2} $\cdot$ d^{-1} until DOY 296 in 2003 [Fig. 4(a)]. For both years, the MODIS GPP rose above that level around DOY 100. Both BigFoot and MODIS GPP dropped off below 1.0 gC $\cdot$ m^{-2} $\cdot$ d^{-1} around DOY 300. The nongrowing season level of the MODIS FPAR was similar (0.2) in both years but only rose

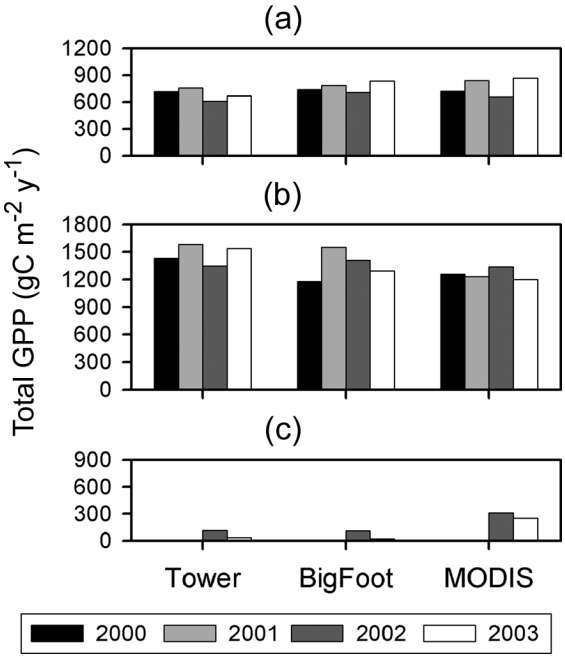

Fig. 5. Interannual variation in total GPP for flux tower, BigFoot, and MODIS. For the BigFoot and MODIS cases, values are averages of 25 1-km^2 MODIS cells. (a) NOBS. (b) HARV. (c) SEVI.

significantly above 0.2 in 2002 [Fig. 4(b)]. $S_{T\,min}$ restricted the MODIS GPP outside the interval of DOY 100–300 [Fig. 4(d)] and S_{VPD} correctly reduced MODIS GPP during a dry period in 2002 around DOY 240 [Fig. 3(e)]. Total GPP was lower in 2003 than in 2002 for both BigFoot and MODIS products but the absolute magnitude was consistently higher for the MODIS products (Fig. 5).

IV. Discussion

A. Boreal Forest Site

Because an increasing growing season length at high latitudes is an expected consequence of projected global warming, and has been inferred from remote sensing [34], it is important to establish the degree to which satellite-based algorithms are able to detect variation in the beginning of the growing season. Winter dormancy in cold-tolerant conifers is broken by warming temperatures rather than photoperiod [35]. The $S_{T\,min}$ in the MOD17 algorithm is not a heat sum approach as is used in more complex phenology models [36], [37]. However, it gives the algorithm sensitivity to low temperatures and it appears to be correctly parameterized for the NOBS site (i.e., a linear ramp from 0 to 1 between -8 °C and $+8.3$ °C).

The MODIS FPAR shows artificial variation during the winter at NOBS, but the variation does not influence GPP much because $S_{t\,min}$ already has ε_g reduced to zero most of the time. FPAR generally drops to about 0.2 in the spring before a sustained rise. This rise is very abrupt and probably is associated with snow melt and exposure of the ground. It is not known to what degree the spring rise of MODIS FPAR is driven by green up of mosses versus the leafing out of local deciduous species. Isolating the relative contributions of ground reflectance and green leaf area would require sustained and

extensive observations that were not logistically feasible in this study.

In boreal forests, the decline in incident PAR at the end of the growing season places an especially strong constraint on GPP. Decreasing photoperiod as well as nighttime temperatures below 0 °C act as a signal to induce the physiological processes of dormancy and hardening [38]. The hardening process permits conifer foliage to tolerate cold winter temperatures but also reduces metabolic rates and, hence, photosynthetic capacity. Modeling the decline of GPP at the end of the growing season at NOBS is relatively easy because of the strong dependence on temperature and ↓PAR; the general trend is captured well by the BigFoot and MODIS GPP. The GPP falloff to zero was significantly earlier in 2002 than in the other years in the tower GPP (DOY 280 versus ∼DOY 300 in other years). That anomaly was captured by the MODIS product because $S_{T\,min}$ was also relatively low during October [Fig. 2(d)].

That the signs of the year-to-year changes in total GPP were the same at NOBS for the flux tower and MODIS estimates suggests that the MODIS algorithm is effective in detecting these changes. The temperature signal, FPAR signal, and ↓PAR signal all contributed to the low GPP estimate for 2002. In a similar study at a different boreal forest flux tower site, output from an LUE model (VPM) did not show agreement in the sign of the interannual variation in total GPP and this problem was attributed in part to the parameterization of the minimum temperature scalar [39]. The growing abundance of multiyear flux tower data will make it increasingly feasible to test and parameterize $S_{T\,min}$ directly from field measurements.

B. Deciduous Broadleaf Forest Site

For deciduous forest species, the renewal of GPP in spring is constrained by recovery of leaf area. Bud burst is dependent on prolonged exposure to temperatures above a certain threshold [40] but also, in some cases, requires long days [41]. At HARV, $S_{T\,min}$ helps account for this temperature factor and FPAR tracks leaf out. Generally, the spring rise in MODIS FPAR at HARV tends to run a week or more earlier than the spring rise in the BigFoot FPAR trajectory. This bias is seen for all years and is probably associated with the leafing out of vernal herbs and understory trees [42], [43] which would be detected by the MODIS sensor but not by the measurements of above- and below-canopy PAR that were used to create the BigFoot LAI trajectory.

The end of the growing season in deciduous forests is, likewise, driven by photoperiod and low temperatures, but can also be influenced by soil drought [38]. Leaf senescence and leaf fall at HARV were unusually late in 2002 based on the observations at the flux tower [32]. This phenological anomaly did not have a corresponding effect on tower GPP, which fell to near zero by the end of October in all four years. The relatively late leaf fall in 2002 is evident in the MODIS FPAR but it did not significantly affect October GPP because ↓PAR and $S_{T\,min}$ are already so low during late October.

In contrast to the NOBS site, the sign of the change in total GPP from year to year differed between the flux tower and MODIS products at the HARV site. Another difference was that the range of the MODIS total GPP was smaller rather than larger. This kind of discrepancy at the HARV site is not unique to results from the MOD17 model [44] and probably relates to multiple factors. One factor in the MODIS algorithm that probably contributed to these differences relates to oversensitivity of MOD17 to VPD (a linear ramp from 1 to 0 over the VPD range of 650–3100 Pa). This effect was evident from the low S_{VPD} during midsummer of 2001 [Fig. 3(e)]. Neither the BigFoot GPP nor the tower GPP [45] showed a sustained depression in GPP during that period, which is also consistent with the conclusion from leaf level analyses that photosynthesis at the HARV site is not very sensitive to VPD [46].

C. Grassland Site

At the desert grassland site, the build-up of green LAI/FPAR following the beginning of monsoon rains is a function of rapid recovery of bryophytes and lichens, germination and growth of annuals (released from dormancy by leaching of germination inhibitors), and regrowth of foliage in perennial bunchgrasses [47]. In 2002, precipitation was near normal, with large precipitation events around DOY 200 that were associated with greening up and significant GPP. The year 2003 also had precipitation events starting around DOY 200 but they were of much lower magnitude and with correspondingly less GPP [Fig. 4(a)]. MODIS FPAR captured the beginning of the growing season well in 2002, rising from about 0.2 to 0.4, but it showed virtually no increase from a background mean of about 0.2 in 2003.

The incident PAR, FPAR, and Tmin inputs to the MODIS GPP algorithm helped it correctly shut down GPP at the end of the growing season at SEVI. There was also agreement between the MODIS estimates and the ground-based estimates on the sign and magnitude of the difference in annual GPP between the 2002 and 2003. However, there is clearly a problem with the MODIS product regarding the absolute magnitude of annual GPP. MODIS FPAR never fell below about 0.2, which results in substantial GPP even when conditions appeared to be too dry to support much metabolic activity. MODIS FPAR also remains about 0.2 throughout the year at the BigFoot agricultural site in Illinois [21], a pattern that is clearly incorrect.

D. Prospects for Monitoring Interannual Variation in GPP

Results of assessing interannual variation in MODIS GPP at these three sites support the general approach of integrating reflectance data (i.e., FPAR) and climate data with an LUE model to monitor interannual variation in GPP. At high latitudes, the strong control of temperature and light on GPP contributes to the success of the relatively simple MOD17 algorithm in simulating GPP. At midlatitudes, the growing season length is a strong determinant of total annual GPP [48] and the seasonality of FPAR helps capture that. However, the MOD17 algorithm did not do well in simulating the interannual variation in annual GPP at the HARV site suggesting a closer look at all algorithm components and inputs is needed [8], [44]. At a midlatitude grassland site, interannual difference in FPAR and climate are likely to be strong enough to indicate the correct sign of changes in total GPP, however, problems with the FPAR outside the growing season need to be resolved.

V. Conclusion

The combination of information on FPAR and daily climate in a light use efficiency-based model is an effective means of estimating daily GPP at large spatial scales. Interannual variation in leaf phenology is clearly detected by the MODIS FPAR in some cases. Interannual variation in the minimum temperature and VPD scalars that down regulate light use efficiency is also evident. Both the FPAR and climate factors are contributing to the success (albeit limited in some cases) of the MOD17 algorithm in capturing interannual variation in GPP at these sites. Increased attention to estimates of FPAR while it is at low levels outside the growing season, and to parameterization of the minimum temperature and VPD scalars for particular vegetation types, will contribute to improved performance of the MODIS GPP algorithm.

Acknowledgment

The authors would like to thank the Harvard LTER site and the Sevilleta LTER sites for the use of their facilities. Data available through AmeriFlux, FLUXNET, and the ORNL DAAC Mercury Data System were essential to this study. The authors would also like to thank J. O'Keefe (Harvard University) for consultation on the Harvard Forest phenology data.

References

[1] R. H. Waring, B. E. Law, M. L. Goulden, S. L. Bassow, R. W. McCreight, S. C. Wofsy, and F. A. Fazzaz, "Scaling gross ecosystem production at Harvard Forest with remote sensing: A comparison of estimates from a constrained quantum-use efficiency model and eddy correlation," *Plant, Cell, Environ.*, vol. 18, pp. 1201–1213, 1995.

[2] J. Roy and B. Saugier, "Terrestrial primary productivity: definitions and milestones," in *Terrestrial Global Productivity*, J. Roy, B. Saugier, and H. A. Mooney, Eds. San Diego, CA: Academic, 2001, pp. 1–6.

[3] R. R. Nemani, C. D. Keeling, H. Hashimoto, W. M. Jolly, S. C. Piper, C. J. Tucker, R. B. Myneni, and S. W. Running, "Climate-driven increases in global terrestrial net primary production from 1982 to 1999," *Science*, vol. 300, pp. 1560–1563, 2003.

[4] S. W. Running, R. R. Nemani, F. A. Heinsch, M. Zhao, M. Reeves, and H. Hashimoto, "A continuous satellite-derived measure of global terrestrial production," *BioScience*, vol. 54, pp. 547–560, 2004.

[5] S. R. Running, D. D. Baldocchi, D. P. Turner, S. T. Gower, P. S. Bakwin, and K. A. Hibbard, "A global terrestrial monitoring network integrating tower fluxes, flask sampling, ecosystem modeling and EOS satellite data," *Remote Sens. Environ.*, vol. 70, pp. 108–128, 1999.

[6] D. P. Turner, S. Ollinger, M. L. Smith, O. Krankina, and M. Gregory, "Scaling net primary production to a MODIS footprint in support of Earth Observing System product validation," *Int. J. Remote Sens.*, vol. 25, pp. 1961–1979, 2004.

[7] M. L. Goulden, J. W. Munger, S. Fan, B. C. Daube, and S. C. Wofsy, "Measurements of carbon sequestration by long-term eddy covariance: Methods and a critical evaluation of accuracy," *Global Change Biol.*, vol. 2, pp. 169–182, 1996.

[8] D. P. Turner, W. D. Ritts, W. B. Cohen, S. T. Gower, M. Zhao, S. W. Running, S. C. Wofsy, S. Urbanski, A. Dunn, and J. W. Munger, "Scaling gross primary production (GPP) over boreal and deciduous forest landscapes in support of MODIS GPP product validation," *Remote Sens. Environ.*, vol. 88, pp. 256–270, 2003.

[9] R. B. Myneni, R. R. Nemani, and S. W. Running, "Estimation of global leaf area index and absorbed PAR using radiative transfer models," *IEEE Trans. Geosci. Remote Sens.*, vol. 35, no. 6, pp. 1380–1393, Nov., 1997.

[10] R. Myneni, R. Hoffman, Y. Knyazikhin, J. Privette, J. Glassy, and H. Tian, "Global products of vegetation leaf area and fraction absorbed PAR from one year of MODIS data," *Remote Sens. Environ.*, vol. 76, pp. 139–155, 2002.

[11] S. D. Schubert, R. B. Rood, and J. Pfaendtner, "An assimilated dataset for earth science applications," *Bull. Amer. Meteorol. Soc.*, vol. 74, pp. 2331–2342, 1993.

[12] S. W. Running, P. E. Thornton, R. Nemani, and J. M. Glassy, "Global terrestrial gross and net primary productivity from the Earth Observing System," in *Methods in Ecosystem Science*, O. E. Sala, R. B. Jackson, H. A. Mooney, and R. W. Howarth, Eds. New York: Springer-Verlag, 2000, pp. 44–57.

[13] P. J. Sellers *et al.*, "BOREAS in 1997: experiment overview, scientific results, and future directions," *J. Geophys. Res.*, vol. 102, pp. 28 731–28 769, 1997.

[14] S. T. Gower, J. C. Vogel, J. M. Norman, C. J. Kucharik, S. J. Steele, and T. K. Stow, "Carbon distribution and above ground net primary production in aspen, jack pine, and black spruce stands in Saskatchewan and Manitoba, Canada," *J. Geophys. Res.*, vol. 102, pp. 29 029–29 041, 1997.

[15] M. L. Goulden, S. C. Wofsy, J. W. Harden, S. E. Trumbore, P. M. Crill, S. T. Gower, T. Fries, B. C. Daube, S.-M. Fan, D. J. Sutton, A. Bazzaz, and J. W. Munger, "Sensitivity of boreal forest carbon balance to soil thaw," *Science*, vol. 279, pp. 214–217, 1998.

[16] S. C. Wofsy, J. W. Goulden, S.-M. F. Munger, P. S. Bakwin, B. C. Daube, S. L. Bassow, and F. A. Bazzaz, "Net exchange of CO_2 in a midlatitude forest," *Science*, vol. 260, pp. 1314–1317, 1993.

[17] S. A. Kurc and E. E. Small, "Dynamics of evapotranspiration in semiarid grassland and shrubland during the summer monsoon season, central New Mexico," *Water Resources Res.*, vol. 40, no. W09305, 2004. DOI: 10.1029.2004.WR003068.

[18] M. S. Zhao, F. A. Heinsch, R. R. Nemani, and S. W. Running, "Improvements of the MODIS terrestrial gross and net primary production global data set," *Remote Sens. Environ.*, vol. 95, pp. 164–176, 2005.

[19] EDC. (2004) USGS EROS Data Center. [Online]. Available: http://redhook.gsfc.nasa.gov/~imswww/pub/imswelcome/plain.html

[20] P. B. Reich, D. P. Turner, and P. Bolstad, "An approach to spatially distributed modeling of net primary production (NPP) at the landscape scale and its application in validation of EOS NPP products," *Remote Sens. Environ.*, vol. 70, pp. 69–81, 1999.

[21] D. P. Turner, W. D. Ritts, W. B. Cohen, T. Maeirsperger, S. T. Gower, A. Kirschbaum, S. W. Running, M. Zhao, S. C. Wofsy, A. Dunn, B. E. Law, J. L. Campbell, W. Oechel, H. Kwon, T. P. Meyers, E. E. Small, S. A. Kurc, and J. A. Gamon, "Site-level evaluation of satellite-based global terrestrial gross primary production and net primary production monitoring," *Global Change Biol.*, vol. 11, pp. 666–684, 2005.

[22] J. L. Campbell, S. Burrows, S. T. Gower, and W. B. Cohen, "BigFoot: Characterizing land cover, LAI, and NPP at the landscape scale for EOS/MODIS validation," Environ. Sci. Division, Oak Ridge Nat. Lab., Oak Ridge, TN, Field Manual Version 2.1, 1999.

[23] S. T. Gower, C. J. Kucharik, and J. M. Norman, "Direct and indirect estimation of leaf area index, f_{APAR} and net primary production of terrestrial ecosystems," *Remote Sens. Environ.*, vol. 70, pp. 29–51, 1999.

[24] W. B. Cohen, T. K. Maiersperger, S. T. Gower, and D. P. Turner, "An improved strategy for regression of biophysical variables and Landsat ETM+ data," *Remote Sens. Environ.*, vol. 84, pp. 561–571, 2003.

[25] W. B. Cohen, T. K. Maiersperger, Z. Yang, S. T. Gower, D. P. Turner, W. D. Ritts, M. Berterretche, and S. W. Running, "Comparisons of land cover and LAI estimates derived from ETM+ and MODIS for four sites in North America: A quality assessment of 2000/2001 provisional MODIS products," *Remote Sens. Environ.*, vol. 88, pp. 233–255, 2003.

[26] W. B. Cohen, T. K. Maiersperger, D. P. Turner, W. D. Ritts, D. Pflugmacher, R. E. Kennedy, A. Kirschbaum, S. W. Running, M. Costa, and S. T. Gower, "MODIS land cover and LAI collection 4 product quality across nine sites in the Western Hemisphere," *IEEE Trans. Geosci. Remote Sens.*, vol. 44, no. 7, pp. 1843–1857, Jul. 2006.

[27] S. W. Running, "Testing FOREST-BGC ecosystem process simulations across a climatic gradient in Oregon," *Ecol. Appl.*, vol. 4, pp. 238–247, 1994.

[28] J. S. Kimball, A. R. Keyser, S. W. Running, and S. S. Saatchi, "Regional assessment of boreal forest productivity using an ecological process model and remote sensing parameter maps.," *Tree Physiol.*, vol. 20, pp. 761–775, 2000.

[29] G. Wohlfahrt, M. Bahn, A. Haslwanter, C. Newesely, and A. Cernusca, "Estimation of daytime ecosystem respiration to determine gross primary production of a mountain meadow," *Agricult. Forest Meteorol.*, vol. 130, pp. 13–25, 2005.

[30] M. Gockede, C. Rebmann, and T. Foken, "A combination of quality assessment tools for eddy covariance measurements with footprint modeling for the characterization of complex sites," *Agricult. Forest Meteorol.*, vol. 127, pp. 175–188, 2004.

[31] K. R. Wythers, P. B. Reich, and D. P. Turner, "Predicting leaf area index from scaling principles: Corroboration and consequences," *Tree Physiol.*, vol. 23, pp. 1171–1179, 2003.

[32] J. O'Keefe, "Phenology of woody species,", 2004. [Online]. Available: http://harvardforest.fas.harvard.edu/data/p00/hf003/hf003.html..
[33] J. S. Kimball, P. E. Thornton, M. A. White, and S. W. Running, "Simulating forest productivity and surface-atmosphere carbon exchange in the BOREAS study region," *Tree Physiol.*, vol. 17, pp. 589–599, 1997.
[34] R. B. Myneni, C. D. Keeling, C. D. Tucker, G. Asrar, and R. R. Nemani, "Increased plant growth in the northern high latitudes from 1981–1991," *Nature*, vol. 386, pp. 698–702, 1997.
[35] T. Lundmark, J.-E. Hallgren, and J. Heden, "Recovery from winter depression of photosynthesis in pine and spruce," *Trees*, vol. 2, pp. 110–114, 1988.
[36] S. E. Frolking, M. L. Goulden, S. C. Wofsy, S.-M. Fan, D. J. Sutton, J. W. Munger, A. M. Bazzaz, B. C. Daube, P. M. Crill, J. D. Aber, L. E. Band, X. Wang, K. Savage, T. R. Moore, and R. C. Harriss, "Modeling temporal variability in the carbon balance of a spruce/moss boreal forest," *Global Change Biol.*, vol. 2, pp. 343–366, 1996.
[37] M. A. White, P. E. Thornton, and S. W. Running, "A continental phenology model for monitoring vegetation responses to interannual climatic variability," *Global Biogeochem. Cycles*, vol. 11, pp. 217–234, 1997.
[38] P. J. Kramer and T. T. Kozlowski, *Physiology of Woody Plants*. New York: Academic, 1979.
[39] X. Xiao, D. Hollinger, J. Aber, M. Goltz, E. A. Davidson, Q. Zhang, and B. Moore, III, "Satellite-based modeling of gross primary production in an evergreen needleleaf forest," *Remote Sens. Environ.*, vol. 89, pp. 519–534, 2004.
[40] M. G. R. Cannell, "Modeling the phenology of trees," in *Modeling to Understand Forest Functions*, H. Jozefek, Ed. Joensuu, Finland: Univ. Joensuu, 1990, pp. 11–27.
[41] O. M. Heide, "Daylength and thermal time responses of bud burst during dormancy release in some northern deciduous trees," *Physiol. Plantarum*, vol. 88, pp. 531–540, 1993.
[42] E. L. Braun, *Deciduous Forests of Eastern North America*. New York: Hafner, 1950.
[43] C. K. Augspurger and E. A. Bartlett, "Differences in leaf phenology between juvenile and adult trees in a temperate deciduous forest," *Tree Physiol.*, vol. 23, pp. 517–525, 2003.
[44] X. Xiao, Q. Zhang, B. H. Braswell, S. Urbanski, S. Boles, S. C. Wofsy, B. Moore, III, and D. Ojima, "Modeling gross primary production of temperate deciduous broadleaf forest using satellite images and climate data," *Remote Sens. Environ.*, vol. 91, pp. 256–270, 2004.
[45] D. P. Turner, S. Urbanski, S. C. Wofsy, D. J. Bremer, S. T. Gower, and M. Gregory, "A cross-biome comparison of light use efficiency for gross primary production," *Global Change Biol.*, vol. 9, pp. 383–395, 2003.
[46] S. L. Bassow and F. A. Bazzaz, "How environmental conditions affect canopy leaf-level photosynthesis in four deciduous tree species," *Ecology*, vol. 79, pp. 2660–2675, 1998.
[47] H. Lambers, F. S. Chapin, III, and L. P. Thijs, *Plant Physiological Ecology*. New York: Springer-Verlag, 1998.
[48] M. L. Goulden, J. W. Munger, S.-M. Fan, B. C. Daube, and S. C. Wofsy, "Exchange of carbon dioxide by a deciduous forest: Response to interannual climate variability," *Science*, vol. 271, pp. 1576–1578, 1996.

David. P. Turner received the Ph.D. degree in botany from Washington State University, Pullman, in 1984.

He is currently an Associate Professor in the Forest Science Department, Oregon State University, Corvallis. His research interests are in the area of remote sensing and ecological modeling.

William David Ritts received the M.S. degree in natural resource planning from Humboldt State University, Arcata, CA, in 2003.

He is currently a Faculty Research Assistant in the Forest Science Department, Oregon State University, Corvallis, working on the development and application of spatially distributed carbon cycle models.

Maosheng Zhao received the Ph.D. degree in climatology from the Institute of Atmospheric Physics, Chinese Academy of Sciences, Beijing, in 2001.

He is currently a Postdoctoral Researcher and Primary Software Engineer, Numerical Terradynamic Simulation Group, t University of Montana, Missoula.

Shirley A. Kurc received the B.A. degree in mathematics from Kalamazoo College, Kalamazoo, MI, in 1994. She is currently pursuing the Ph.D. degree ath the University of Colorado, Boulder.

Her research interests include eco-hydrology, surface water, fluid mechanics, and numerical methods in hydrology.

Allison L. Dunn received the Ph.D. degree in earth and planetary sciences from Harvard University, Cambridge, MA, in 2006.

She is currently a Postdoctoral Fellow with a joint appointment at the University of Manitoba, Winnipeg, MB, Canada, and Harvard University. Her research interests are atmosphere–biosphere interactions and terrestrial carbon cycling.

Steven C. Wofsy received the Ph.D. degree in chemistry from Harvard University, Cambridge, MA, in 1971.

He is the Abbott Lawrence Rotch Professor of Atmospheric and Environmental Science at Harvard University. His research interests include atmospheric chemistry and the role of the biosphere in the terrestrial carbon cycle.

Eric E. Small received the Ph.D. degree in earth science from the University of California, Santa Cruz, in 1998.

He is currently an Assistant Professor with the Department of Geological Sciences, University of Colorado, Boulder. His research interests include the hydrology of semiarid ecosystems and land–atmosphere interactions.

Steven W. Running received the B.S. degree in botany and the M.S. degree in forest management from Oregon State University, Corvallis, and the Ph.D. degree in forest ecophysiology from Colorado State University, Fort Collins, in 1972, 1973, and 1979, respectively.

He is currently a Professor of ecology and the Director of the Numerical Terradynamics Simulation Group, University of Montana, Missoula.